Structure−Reactivity Relationships of Amido-Pyridine-Supported Rare-Earth-Metal Alkyl Complexes

Melanie Zimmermann,[†] Karl W. Törnroos,[†] Robert M. Waymouth,*[,‡] and Reiner Anwander*[,†]

Department of Chemistry, University of Bergen, Allégaten 41, 5007 Bergen, Norway, and Chemistry Department, Stanford University, Stanford, California 94305

Received November 28, 2007

Treatment of rare-earth-metal dialkyl complexes with group 13 cocatalysts is a prominent approach to generate homogeneous catalysts active in olefin polymerization. Reaction of $Ln(CH_2SiMe_3)_3(THF)_2$ with monovalent imino-amido-pyridine [2-{(2,6-*i*$Pr_2C_6H_3$)N═CMe}-6-{(2,6-*i*$Pr_2C_6H_3$)NHCMe$_2$}C_5H_3N] (H**L$_2$**) gives donor solvent-free discrete dialkyl compounds [**L$_2$**]$Ln(CH_2SiMe_3)_2$ (Ln = Sc, Y, Lu). In the solid state the scandium derivative is isostructural to the previously reported lutetium complex (Gordon et al.). Activation by borate cocatalysts $[Ph_3C][B(C_6F_5)_4]$ and $[PhNMe_2H][B(C_6F_5)_4]$ produces ion pairs that polymerize ethylene in moderate yields (activity: Sc > Lu). Cationization with *N*-[tris(pentafluorophenyl)borane]-3*H*-indole gives inactive species. $^1H/^{13}C/^{11}B/^{19}F$ NMR spectroscopy is applied to examine the interaction of the rare-earth-metal dialkyl complexes with the boron cocatalysts. In contrast to the monoalkyl diamido-pyridine compounds [**L$_1$**]$Ln(CH_2SiMe_3)(THF)_x$ (H**L$_1$** = [2,6-{(2,6-*i*$Pr_2C_6H_3$)NH-CH_2}C_5H_3N], the dialkyl imino-amido-pyridine complexes do not polymerize methyl methacrylate.

Much of the recent interest in organolanthanide chemistry is linked to the academic and industrial quest for novel types of olefin polymerization catalysts.[1] Improvement of the overall catalytic performance is by its very nature related to ancillary ligand design and the generation of highly electron deficient metal centers (*metal cationization*). While cyclopentadienyl and related carbocyclic ligand environments (e.g., indenyl) have yielded a number of isolable and active catalysts, the rich coordination chemistry of the lanthanides provides considerable opportunities for further ligand design and optimization.[2] Nitrogen (imines, amides) and oxygen donor ligands (alkoxides) have proven to be versatile components of polydentate ligands for lanthanide polymerization catalysts. **N**-type (amide, imine) ligands have been successfully employed for the synthesis of discrete organorare-earth-metal complexes; nevertheless the number of reported active catalyst systems remains limited.[1b] Chart 1 depicts representative **N**-type (amide, imine) catalyst precursors for ethylene polymerization (Table 2).[3−8] Typically, these complexes contain at least two alkyl ligands and only become active for polymerization upon activation by organoboron and/or organoaluminum cocatalysts.

Chart 1. Rare-Earth-Metal Bis(alkyl) Complexes with N-Type Ancillary Ligands, Active in Ethylene Polymerization upon Addition of Activators (cf., Table 2)

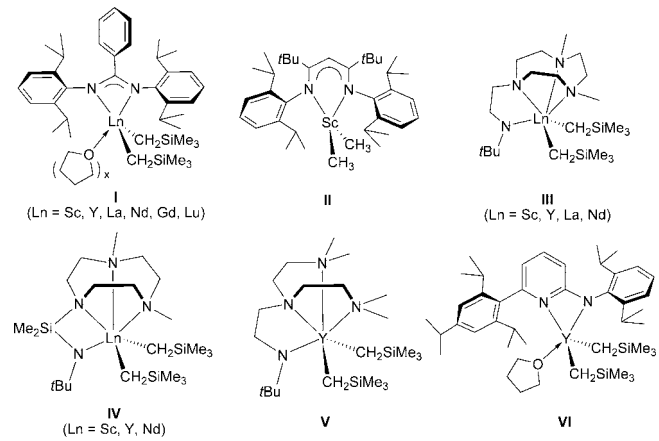

Due to their successful application as ligands for group 4 chemistry,[9] we investigated the coordination chemistry of the diamido-pyridine ligands of the $[NNN]^{2-}$ type (**L$_1$**, Chart 2) for organorare-earth-metal chemistry.[10] The influence of ligand modifications (aryl substituents, donor atoms) and the effect of

* To whom correspondence should be addressed. Fax: (+47) 5558-9490. E-mail: reiner.anwander@kj.uib.no.
[†] University of Bergen.
[‡] Stanford University.

(1) For reviews see: (a) Hou, Z.; Wakatsuki, Y. *Coord. Chem. Rev.* **2002**, *231*, 1. (b) Gromada, J.; Carpentier, J. F.; Mortreux, A. *Coord. Chem. Rev.* **2004**, *248*, 397. (c) Hyeon, J. Y.; Gottfriendsen, J.; Edelmann, F. T. *Coord. Chem. Rev.* **2005**, *249*, 2787. (d) Zeimentz, P. M.; Arndt, S.; Elvidge, B. R.; Okuda, J. *Chem. Rev* **2006**, *106*, 2404, and references therein.

(2) For recent reviews see: (a) Piers, W. E.; Emslie, D. J. H. *Coord. Chem. Rev.* **2002**, *233−234*, 131. (b) Gibson, V. C.; Spitzmesser, S. K. *Chem. Rev.* **2003**, *103*, 283.

(3) (a) Bambirra, S.; Bouwkamp, M. W.; Meetsma, A.; Hessen, B. *J. Am. Chem. Soc.* **2004**, *126*, 9182. (b) Bambirra, S.; van Leusen, D.; Meetsma, A.; Hessen, B.; Teuben, J. H. *Chem. Commun.* **2003**, 522. (c) Bambirra, S.; Otten, E.; van Leusen, D.; Meetsma, A.; Hessen, B. *Z. Anorg. Allg. Chem.* **2006**, *632*, 1950. (d) Bambirra, S.; Meetsma, A.; Hessen, B. *Organometallics* **2006**, *25*, 3454.

(4) Hayes, P. G.; Piers, W. E.; McDonald, R. *J. Am. Chem. Soc.* **2002**, *124*, 2132.

(5) Bambirra, S.; van Leusen, D.; Meetsma, A.; Hessen, B.; Teuben, J. H. *Chem. Commun.* **2001**, 637.

(6) Bambirra, S.; van Leusen, D.; Tazelaar, C. G. J.; Meetsma, A.; Hessen, B. *Organometallics* **2007**, *26*, 1014.

(7) Bambirra, S.; Boot, S. T.; van Leusen, D.; Meetsma, A.; Hessen, B. *Organometallics* **2004**, *23*, 1891.

(8) Kretschmer, W. P.; Meetsma, A.; Hessen, B.; Schmalz, T.; Qayyum, S.; Kempe, R. *Chem.−Eur. J.* **2006**, *12*, 8969.

(9) (a) Guérin, F.; McConville, D. H.; Payne, N. C. *Organometallics* **1996**, *15*, 5085. (b) Guérin, F.; McConville, D. H.; Vittal, J. J. *Organometallics* **1996**, *15*, 5586.

(10) Estler, F.; Eickerling, G.; Herdtweck, E.; Anwander, R. *Organometallics* **2003**, *22*, 1212.

10.1021/om701195x CCC: $40.75
Publication on Web 08/16/2008

Chart 2. Dianionic $[NNN]^{2-}$ and Monoanionic $[NNN]^{-}$ Ligand Precursors

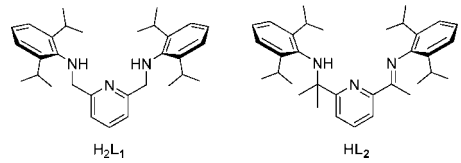

Scheme 1. Synthesis of $[L_1]Ln(CH_2SiMe_3)(THF)_x$ (2) and $[L_2]Ln(CH_2SiMe_3)_2$ (3) by Alkane Elimination

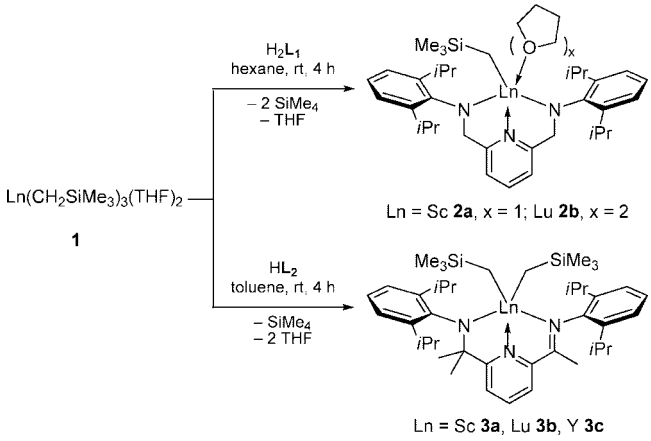

the lanthanide metal size revealed that the catalytic activity is sensitively balanced by steric and electronic factors.[10,11] Monoanionic imino-amido-pyridine ligands ($\mathbf{L_2}$, Chart 1) yield late transition metal catalysts active for ethylene polymerization[12] but also enabled the synthesis of discrete conformationally rigid lanthanide complexes.[13,14] The $[\mathbf{NNN}]^-$ ligand $\mathbf{L_2}$, a monoanionic analogue of its dianionic congener $\mathbf{L_1}$, retains the characteristic features of the pyridine ligand backbone and the (aryl)substitution pattern at the amido/imino functionality, enabling a direct comparison of steric and electronic properties of lanthanide complexes derived from sterically similar monoanionic or dianionic ligand environments.

Herein, we describe structure−reactivity relationships of rare-earth-metal (Ln) alkyl complexes bearing diamido-pyridine ($\mathbf{L_1}$) and imino-amido-pyridine ligands ($\mathbf{L_2}$) and their performance as catalyst precursors for ethylene polymerization, giving special consideration to the impact of the Ln^{3+} size and the type of cocatalyst.

Results and Discussion

Synthesis and Characterization of $[L_1]Ln(CH_2SiMe_3)(THF)_x$ and $[L_2]Ln(CH_2SiMe_3)_2$. Mono(alkyl)diamidopyridine complexes $[\mathbf{L_1}]Ln(CH_2SiMe_3)(THF)_x$ (Ln = Sc, x = 1 (**2a**); Lu, x = 2 (**2b**)) were prepared according to an alkane elimination reaction from $H_2\mathbf{L_1}$ and $Ln(CH_2SiMe_3)_3(THF)_2$ in hexane as described previously (Scheme 1).[10] The trialkyl $Ln(CH_2SiMe_3)_3(THF)_2$ (Ln = Sc (**1a**), Lu (**1b**), and Y (**1c**)) reacts similarly with light yellow [2-{(2,6-iPr$_2$C$_6$H$_3$)N=CMe}-6-{(2,6-iPr$_2$C$_6$H$_3$)NHCMe$_2$}-C$_5$H$_3$N] ($H\mathbf{L_2}$) with release of $SiMe_4$ and THF to form donor solvent-free compounds $[\mathbf{L_2}]Ln(CH_2SiMe_3)_2$ (**3**) (Scheme 1, procedure described by Gordon).[13] An instantaneous color change of the reaction mixture to dark red evidenced the coordination of the monoanionic imino-amido ligand to the lanthanide metal center. Upon removal of the solvent and the volatile reaction byproducts, dark red powdery complexes **3** were obtained with yields decreasing with increasing Ln^{3+} size (Ln = Sc, 92%; Lu, 52%; Y, 32%).

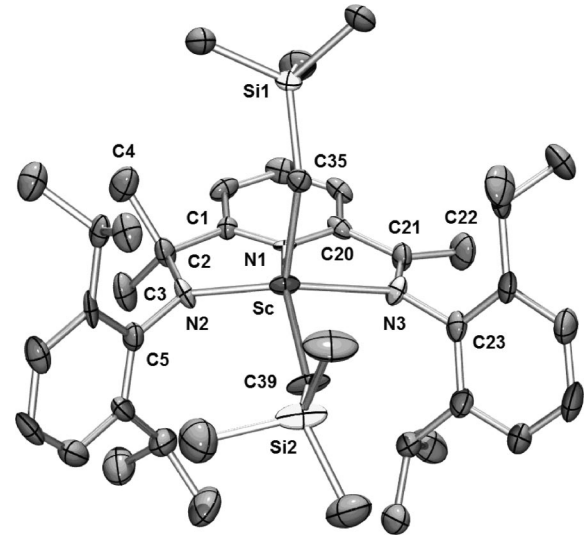

Figure 1. Molecular structure of **3a** (atomic displacement parameters set at the 50% level). Hydrogen atoms and solvent are omitted for clarity. Selected bond distances [Å] and angles [deg]: Sc−N1 2.245(9), Sc−N2 2.103(9), Sc−N3 2.436(9), Sc−C35 2.23(1), Sc−C39 2.25(1), N2−C2 1.48(2), N3−C21 1.31(2), C2−C3 1.52(2), C2−C4 1.56(2), C1−C2 1.51(2), C20−C21 1.49(2); N1−Sc−N2 72.3(3), N1−Sc−N3 67.6(3), N2−Sc−N3 134.1(3), N1−Sc−C35 103.4(3), N1−Sc−C39 145.3(4), C35−Sc−C39 107.6(5), N2−Sc−C35 111.5(4), N2−Sc−C39 109.4(5), N3−Sc−C35 99.0(4), N3−Sc−C39 92.1(4), C1−C2−N2 108.1(9), C20−C21−N3 116.1(10), C20−C21−C22 119.9(11), Sc−N2−C5 121.0(7), Sc−N3−C23 124.2(7).

The IR spectra of complexes **3** show a strong absorption at 1582 cm^{-1} attributed to the stretching vibration of a metal-coordinated imino group ($H\mathbf{L_2}$: 1644 cm^{-1}). Similar shifts were observed in imino-amido pyridine complexes $[\mathbf{L_2}]Ln(AlMe_4)_2$.[14] Due to the insolubility in aliphatic solvents and low solubility in benzene, NMR spectroscopic investigations of compounds **3** were performed in chlorinated solvents. The ^{1}H NMR spectra of complexes **3** in CD_2Cl_2 at ambient temperature show a highly fluxional behavior even for the smallest metal center, scandium. Cooling to −50 °C, however, revealed ^{1}H and ^{13}C NMR spectra in accordance with the solid state structure. Three singlets at 2.35 ppm (3 H), 1.64 ppm (3 H), and 1.10 ppm (3 H) (**3a**) are characteristic of the imino and amido functionalities of the pyridine ligand backbone (**3c**: 2.36, 1.71, and 1.33 ppm). The presence of four multiplets for the methine groups (ArC*H*Me$_2$) indicates a large rotational barrier for the aryl groups around the N−C$_{ipso}$ bond at low temperature. As reported by Gordon[13] for the lutetium derivative, the ^{1}H NMR spectrum of yttrium complex **3c** shows four distinct resonances for the α-C*H*$_2$ of the neosilylalkyl ligands. Surprisingly, the scandium complex **3a** revealed only two α-C*H*$_2$ resonances at low temperature. However, an X-ray structure analysis of the latter Sc compound **3a** (dark red single crystals were obtained from a saturated benzene solution at −30 °C) proved it to be isostructural to the previously reported lutetium derivative **3b** (Figure 1).[13]

(11) Zimmermann, M.; Estler, F.; Herdtweck, E.; Törnroos, K. W.; Anwander, R. *Organometallics* **2007**, *26*, 6029.
(12) Britovsek, G. J. P.; Gibson, V. C.; Mastroianni, S.; Oakes, D. C. H.; Redshaw, C.; Solan, G. A.; White, A. J. P.; Williams, D. J. *Eur. J. Inorg. Chem.* **2001**, 431.
(13) Cameron, T. M.; Gordon, J. C.; Michalczyk, R.; Scott, B. L. *Chem. Commun.* **2003**, 2282.
(14) Zimmermann, M.; Törnroos, K. W.; Anwander, R. *Angew. Chem., Int. Ed.* **2007**, *46*, 3126; *Angew. Chem.* **2007**, *119*, 3187.

The geometry about the five-coordinate rare-earth-metal center is best described as distorted square pyramidal. The Sc atom is located 0.624(6) Å above the least-squares plane defined by the coordinating atoms N1, N2, N3, and C39, which is slightly less than in the corresponding lutetium compound **3b** (0.663 Å).[13] In accordance with the smaller size of the scandium cation, all Sc−N bonds and the Sc−C35/C39 bonds are shortened compared to the lutetium derivative.[10,13] In contrast, the geometry about the scandium metal center in [**L**$_1$]Sc(CH_2SiMe_3)(THF) (**2a**) was described as distorted trigonal bipyramidal with the pyridine nitrogen and the THF occupying the apical positions (N−Sc−O = 156.01(5)°).[10] The N1−Sc−C39 angle as the widest angle in **3a**, however, measures only 145.3(5)°. Further, the ligand bite angle in bis(alkyl) **3a** is slightly smaller than the one found in the solid state structure of **2a** (134.1(3)° vs 137.04(6)°). The Sc−N(amido) (2.102(9) Å (**3a**); av 2.097 Å (**2a**)) and the Sc−C(alkyl) bond lengths (av 2.24(1) Å (**3a**); 2.248(2) Å (**2a**)) are comparable, while the Sc−N(pyridine) distance of 2.245(9) Å in **3a** appears slightly longer than that in **2a** (2.219(1) Å).

At ambient temperature complexes **3** undergo slow thermal decomposition. Monitoring the complex degradation by ^{1}H NMR spectroscopy revealed the protonated ligand precursor H**L**$_2$ and $SiMe_4$ as the only soluble decomposition products (Supporting Information Figure S1). Additionally the formation of a white rare-earth-metal-containing insoluble solid was observed. Pronounced thermal instability was found for the scandium (**3a**) (total decomposition after 24 h at 40 °C) and yttrium (**3c**) compounds (total decomposition after 4 days at 40 °C), while the lutetium derivative (**3b**) appeared to be more stable (decomposition after several weeks). Solids and solutions of **3** in toluene can be stored at −30 °C under argon for several weeks with only traces of decomposition. Decreasing thermal stability with increasing effective size of the metal cation had been found for complexes **2** (Sc > Lu > Y) and was assumed to reflect the "fit" of the ligand to the rare-earth-metal cation.[10]

Mechanistic details of the decomposition pathway, however, remain elusive. Further investigation of the white rare-earth-metal-containing solid was hampered by the insolubility in aliphatic, aromatic, and etheral solvents. Reasonable degradation pathways might include α-H or γ-H elimination from [Ln-CH_2SiMe_3] moieties, as previously proposed for the thermal decomposition of Ln(CH_2SiMe_3)$_3$(THF)$_x$.[15] Alkyl migration to the ligand imino carbon atom—earlier found for the donor-induced cleavage of [**L**$_2$]La($AlMe_4$)$_2$[14] and for related salicylaldimine complexes[16]—was not observed.

Polymerization of Ethylene. The ethylene polymerization behavior of the mono(alkyl) diamido-pyridine complexes [**L**$_1$]Ln(CH_2SiMe_3)(THF)$_x$ (Ln = Sc, x = 1 (**2a**); Lu, x = 2 (**2b**)) and the bis(alkyl) imino-amido-pyridine complexes [**L**$_2$]Ln(CH_2SiMe_3)$_2$ (Ln = Sc (**3a**), Lu (**3b**)) was investigated to assess the effect of the ancillary ligands (**L**$_1$ vs **L**$_2$), metal size, and the cocatalyst on the catalytic performance. In the absence of a cocatalyst neither mono(alkyl)s **2** nor bis(alkyl)s **3** displayed any activity.[17] Interestingly, neutral complexes **2** had previously been found to initiate the polymerization of methyl methacrylate (MMA), but are inactive toward α-olefins.[10]

Scheme 2. Cationization of [L$_2$]Lu(CH_2SiMe_3)$_2$ with B(C_6F_5)$_3$ (the product was characterized by multinuclear NMR spectroscopy)[13]

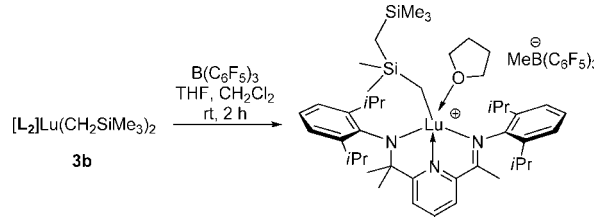

Gordon et al. proved that the [**N**N**N**]$^-$ ligand (**L**$_2$) is suitable to stabilize electron-deficient cationic lanthanide metal centers formed upon B(C_6F_5)$_3$ activation of [**L**$_2$]Lu(CH_2SiMe_3)$_2$ (Scheme 2).[13]

As Gordon et al. had prepared stable cationic Lu derivatives of the [**N**N**N**]$^-$ ligand [**L**$_2$]Lu(CH_2SiMe_3)$_2$ (Scheme 2), [13] we investigated the polymerization behavior of binary catalyst mixtures consisting of lanthanide bis(alkyl) complexes [**L**$_2$]Ln(CH_2SiMe_3)$_2$ and [Ph_3C][B(C_6F_5)$_4$] (**A**), [PhNMe_2H][B(C_6F_5)$_4$] (**B**), or *N*-[tris(pentafluorophenyl)borane]-3*H*-indole (**C**), respectively. Each experiment was performed twice, and representative results are summarized in Table 1 (runs 1−4). Under similar polymerization conditions, the highest activities were observed for the Sc-based initiators (runs 1 and 3), while the lutetium catalysts exhibited slightly lower activity (runs 2 and 4). A similar impact of the lanthanide cation size on the catalytic performance has previously been reported for lanthanide catalysts based on neutral *fac*-κ^3-coordinated [**N**N**N**]^0-type donor ligands {(Me_3[9]aneN_3)Ln(CH_2SiMe_3)$_3$} and {[HC(Me_2pz)$_3$]Ln(CH_2SiMe_3)$_3$} (Sc > Y) as well as the recently reported [(6-amino-6-methyl-1,4-diazepine)Ln-(CH_2SiMe_3)$_3$] (Sc > Y).[18,19]

For further comparison, the ethylene polymerization behavior of the most active rare-earth-metal catalysts based on amido/imino ancillary ligands (Chart 1) are listed in Table 2. The polymerization activities strongly depend on the ancillary ligand, the size of the rare-earth-metal center (Table 2, entries 1−3 and 8−11), polymerization temperatures (Table 2, entries 6, 7, and 14−16), and the cocatalyst/scavenger applied (Table 2, entries 4, 5, and 8−13).

We also observed a dependence of the polymerization activities of precatalysts **3** on the nature of the organoboron cocatalyst. The cocatalyst effect, **A** vs **B**, is more pronounced for initiators **3a**, featuring the smaller scandium center (Table 1, runs 1 and 3). Accordingly, catalyst mixtures containing [PhNMe_2H][B(C_6F_5)$_4$] produced species with higher activity (Table 1, run 3). The coordinating ability of the side-product PhNMe_2 has proven to influence the catalytic performance in several cases[20] and might as well interact with the active species formed by reaction of [**L**$_2$]Ln(CH_2SiMe_3)$_2$ (**3**) and [PhNMe_2H]-[B(C_6F_5)$_4$].

Resconi et al. developed the soluble *N*-[tris(pentafluorophenyl)borane]-3*H*-indole (**C**) as an activator for the polymerization

(15) (a) Schumann, H.; Müller, J. *J. Organomet. Chem.* **1978**, *146*, C5. (b) Schumann, H.; Freckmann, D. M. M.; Dechert, S. *Z. Anorg. Allg. Chem.* **2002**, *682*, 2422. (c) Rufanov, K. A.; Freckmann, D. M. M.; Kroth, H.-J.; Schutte, S.; Schumann, H. *Z. Naturforsch. B: Chem. Sci.* **2005**, *60*, 533.

(16) (a) Emslie, D. J. H.; Piers, W. E.; Parvez, M.; McDonald, R. *Organometallics* **2002**, *21*, 4226. (b) Emslie, D. J. H.; Piers, W. E.; Parvez, M. *Dalton Trans.* **2003**, 2615.

(17) (a) Fryzuk, M. D.; Giesbrecht, G. R.; Rettig, S. J. *Organometallics* **1996**, *15*, 3329. (b) Fryzuk, M. D.; Giesbrecht, G. R.; Rettig, S. J. *Can. J. Chem.* **2000**, *78*, 1003.

(18) Lawrence, S. C.; Ward, B. D.; Dubberley, S. R.; Kozak, C. M.; Mountford, P. *Chem. Commun.* **2003**, 2880.

(19) Ge, S.; Bambirra, S.; Meetsma, A.; Hessen, B. *Chem. Commun.* **2006**, 3320.

(20) Pédeutour, J.-N.; Radhakrishnan, K.; Cramail, H.; Deffieux, A. *Macromol. Rapid Commun.* **2001**, *22*, 1095.

Table 1. Catalytic Ethylene Polymerization at 25 °C

run[a]	precatalyst	cocatalyst[b]	polymer yield [g]	activity [kg/mol bar h][c]	M_n[d]	M_w[d]	M_w/M_n
1	**3a**	**A**	2.60	25	195 800	627 900	3.21
2	**3b**	**A**	1.58	15	213 300	434 800	2.04
3	**3a**	**B**	3.43	33	222 700	822 600	3.69
4	**3b**	**B**	1.39	13	165 200	325 200	1.97
5	**3a**	**C**					
6	**3b**	**C**					

[a] General polymerization procedure: 0.01 mmol of precatalyst, 50 mL of toluene, [cat]/[cocat] = 1:1 (mol/mol), ethylene 150 psi; 1 h, 25 °C. [b] Cocatalyst: **A** = $[Ph_3C][B(C_6F_5)_4]$, **B** = $[PhNMe_2H][B(C_6F_5)_4]$, **C** = *N*-[tris(pentafluorophenyl)borane]-3*H*-indole. [c] Given in kg polymer/(mol Ln atm h). [d] Determined by high-temperature gel permeation chromatography using polyethylene standards.

Table 2. Catalytic Ethylene Polymerization with Complexes Depicted in Chart 1

entry	precatalyst[a]	cocatalyst (equiv)[b]	T [°C]	activity [kg/mol bar h]	M_w ($\times 10^3$)	M_w/M_n	ref
1	I (Ln = Sc)	**B**/TiBAO[c] (1/20)	30	24	93	1.6	3a
2	I (Ln = Y)	**B**/TiBAO[c] (1/20)	30	3006	1666	2.0	3a
3	I (Ln = La)	**B**/TiBAO[c] (1/20)	30	14	470	2.5	3a
4	II	PMAO-IP[d] (20)	50	1200	1866	2.0	4
5	II	$B(C_6F_5)_3$/PMAO-IP[d](1.05/3.33)	50	300	1051	1.7	4
6	III (Ln = Y)	**B** (1)	30	700	471	4.0	5
7	III (Ln = Y)	**B** (1)	80	1790	98	6.0	5
8	IV (Ln = Sc)	**A** (1)	50	75	690	2.2	6
9	IV (Ln = Sc)	**B** (1)	50	145	939	1.7	6
10	IV (Ln = Y)	**A** (1)	50	1343	127	6.6	6
11	IV (Ln = Y)	**B** (1)	50	1280	139	10.5	6
12	V	**A** (1)	50	20	55	2.2	7
13	V	**B** (1)	50				7
14	VI	$[R_2N(CH_3)H][B(C_6F_5)_4]$/TiBAO[c] (1/20)	30	40	68	43.0	8
15	VI	$[R_2N(CH_3)H][B(C_6F_5)_4]$/TiBAO[c] (1/20)	80	1072	67	3.2	8
16	VI	$[R_2N(CH_3)H][B(C_6F_5)_4]$/TiBAO[c] (1/20)	100	808	16	1.4	8

[a] Precatalysts depicted in Chart1. [b] Cocatalyst: **A** = $[Ph_3C][B(C_6F_5)_4]$, **B** = $[PhNMe_2H][B(C_6F_5)_4]$. [c] TiBAO = tetraisobutylalumoxane. [d] PMAO-IP = $AlMe_3$-free methylalumoxane.

Scheme 3. Reaction of $[L_2]Lu(CH_2SiMe_3)_2$ (3b) with A, B, and C

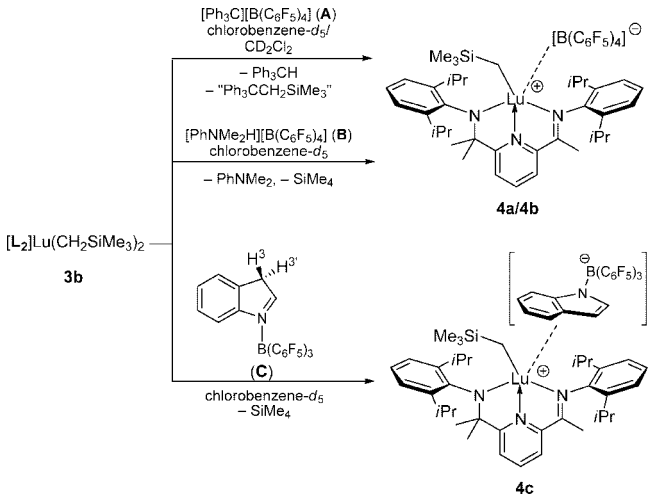

of ethylene.[21] Equimolar mixtures of dimethyl zirconocenes and *N*-[tris(pentafluorophenyl)borane]-3*H*-indole provided significantly higher catalytic activities than systems activated by methylalumoxane (MAO) or $B(C_6F_5)_3/AliBu_3$. *N*-[Tris(pentafluorophenyl)borane]-3*H*-indole, derived from the reaction of indole with $B(C_6F_5)_3$, contains a highly acidic sp^3 carbon (indicated in Scheme 3), generated by a formal N→C hydrogen shift.[22] This soluble proton source provides a convenient method for generating cationic alkyl metallocene precatalysts.[21] However, treatment of $[\mathbf{L_2}]Ln(CH_2SiMe_3)_2$ (**3**) with *N*-[tris(pentaflourophenyl)borane]-3*H*-indole (**C**) did not yield a catalytically active species (Table 1, runs 5 and 6). This distinct polymerization protocol implies a marked influence of the cocatalyst properties, especially the counterion's ability to stabilize and interact with the cationic lanthanide species.

In order to better understand the catalytic activity/inactivity of the catalyst−activator mixtures, we studied equimolar reactions of $[\mathbf{L_2}]Lu(CH_2SiMe_3)_2$ (**3b**) with the borate activators $[Ph_3C][B(C_6F_5)_4]$ (**A**), $[PhNMe_2H][B(C_6F_5)_4]$ (**B**), and *N*-[tris(pentafluorophenyl)borane]-3*H*-indole (**C**) in more detail. Treatment of complex **3b** with 1 equiv of **A** in chlorobenzene-d_5 at 25 °C led to instant formation of a cationic lutetium alkyl species assignable to $\{[\mathbf{L_2}]Lu(CH_2SiMe_3)\}\{B(C_6F_5)_4\}$ (**4a**) as monitored by ^1H, ^{11}B, and ^{19}F NMR spectroscopy (Scheme 3, Figure 2B). The cation formation was accompanied by three organic side-products. While one species could clearly by identified as Ph_3CH (Ph_3CH: δ = 5.56 ppm), the ^1H NMR spectrum features two $SiMe_3$ resonances (0.01 and −0.30 ppm) and two methylene resonances (2.19 and 2.10 ppm) tentatively attributed to "$Ph_3CCH_2SiMe_3$" species. Similar organic byproducts have previously been observed by Mountford et al. when reacting $[Ti(NtBu)(Me_3[9]aneN_3)(CH_2SiMe_3)_2]$ with $[Ph_3C][B(C_6F_5)_4]$.[23] For comparison, the equimolar reaction of $LiCH_2SiMe_3$ and Ph_3CCl was monitored by ^1H NMR spectroscopy in chlorobenzene-d_5, revealing the formation of comparable organic products (Figure 2A).

Despite a detailed investigation of the organic side-products, the actual nature of the two "$Ph_3CCH_2SiMe_3$" species as well as mechanistic details leading to the formation of Ph_3CH remain unknown.[23] The analogous reaction of complex **3b** with 1 equiv of **A** in CD_2Cl_2 at 25 °C produced a complicated mixture of

(21) Guidotti, S.; Camurati, I.; Focante, F.; Angellini, L.; Moscardi, G.; Resconi, L.; Laerdini, R.; Nanni, D.; Mercandelli, P.; Sironi, A.; Beringhelli, T.; Maggioni, D. *J. Org. Chem.* **2003**, *68*, 5445.

(22) Bonazza, A.; Camurati, I.; Guidotti, S.; Mascellari, N.; Resconi, L. *Macromol. Chem. Phys.* **2004**, *205*, 319.

(23) Bolton, P. D.; Clot, E.; Adams, N.; Dubberley, S. R.; Cowley, A. R.; Mountford, P. *Organometallics* **2006**, *25*, 2806.

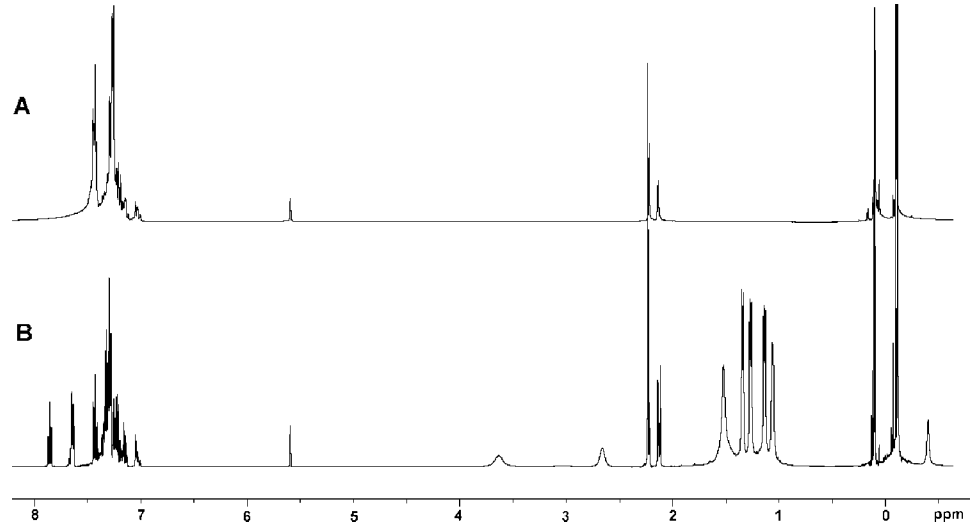

Figure 2. ^{1}H NMR spectra (400.13 MHz) of (A) the equimolar reaction of Ph_3CCl and $LiCH_2SiMe_3$ and (B) **3b**/$[Ph_3C][B(C_6F_5)_4]$ in chorobenzene-d_5 at 298 K.

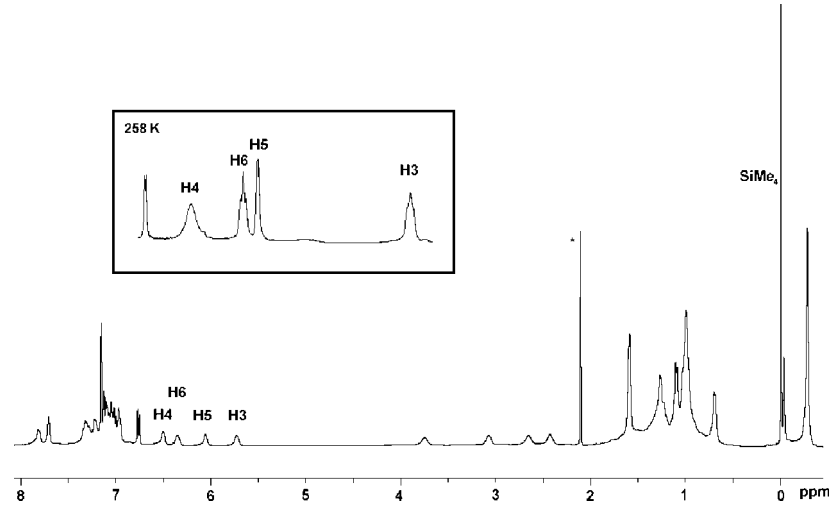

Figure 3. ^{1}H NMR spectrum (400.13 MHz) of **3b**/*N*-[tris(pentafluorophenyl)borane]-3*H*-indole (**C**) in chlorobenzene-d_8 at 298 K (* = toluene residue).

Ph_3CH, "$Ph_3CCH_2SiMe_3$", and other silylated (aliphatic and olefinic) byproducts $[R_xSiMe_y]_n$ (Supporting Information; Figure S2).

^{1}H NMR investigations of the reaction of equimolar amounts of [**L$_2$**]Lu$(CH_2SiMe_3)_2$ (**3b**) and **B** in chlorobenzene-d_5 revealed the formation of an ion pair {[**L$_2$**]Lu(CH_2SiMe_3)}{$B(C_6F_5)_4$} (**4b**), $SiMe_4$, and $PhNMe_2$ (Figure S3, Supporting Information). ^{11}B and ^{19}F NMR spectra substantiate the presence of only one anionic species, the chemical shifts being similar to the ones observed for **4a**. The ^{1}H NMR spectrum, however, shows a highly fluxional behavior of the imino-amido-pyridine ancillary ligand at ambient temperature (Figure S3).

^{1}H NMR spectroscopic investigation of an equimolar **3b**/*N*-[tris(pentafluorophenyl)borane]-3*H*-indole (**C**) mixture in chlorobenzene-d_5 at 25 °C showed the formation of a new species, which we tentatively assigned as {[**L$_2$**]Lu(CH_2SiMe_3)}-{[B(indolyl)$(C_6F_5)_3$]} (**4c**, Scheme 3). The complete disappearance of the diagnostic indole H3/H3′ signals at 2.48 ppm and the formation of $SiMe_4$ indicated the anticipated protonolysis of one $[CH_2SiMe_3]$ ligand by *N*-[tris(pentafluorophenyl)borane]-3*H*-indole. Strikingly, the ^{1}H NMR spectrum features a set of relatively broad resonances between 5.63 and 6.43 ppm assignable to H3, H4, H5, and H6 of the indolyl counterion (Figure 3). These signals show a significant upfield shift compared to the ones found for the separated ion pair $[Ind_2ZrMe][B(indolyl)(C_6F_5)_3]$ (6.37−7.14 ppm)[21] and are in the range of π-coordinated indenyl moieties. These findings suggest a strong interaction of the indolyl π-system with the electron-deficient lutetium metal center. Few previous investigations document the coordination flexibility of indolyl ligands with respect to $\eta^6 \rightarrow \eta^5(\eta^3, \eta^1)$ shifts.[24] Further evidence of extensive steric constraint due to interaction with the counterion is given by the appearance of four multiplets for the methine groups ($ArCHMe_2$: δ = 3.65, 3.14, 2.66, and 2.53 ppm). This indicates a large rotational barrier for the aryl groups around the $N-C_{ipso}$ bond already at 25 °C, while resolution of these signals in [**L$_2$**]Lu$(CH_2SiMe_3)_2$ (**3b**) occurred only at low temperatures (*vide supra*). One single signal in the ^{11}B NMR spectrum corroborates the presence of only one boron-containing species, while the ^{19}F NMR spectrum shows a complicated pattern of 10 resonances, indicating conformational rigidity on the NMR

(24) (a) Evans, W. J.; Brady, J. C.; Ziller, J. W. *Inorg. Chem.* **2002**, *41*, 3340. (b) White, C.; Thompson, S. J.; Maitlis, P. M. *J. Chem. Soc., Dalton Trans.* **1977**, 1654. (c) Chen, S.; Carperos, V.; Noll, B.; Swope, R. J.; DuBois, M. R. *Organometallics* **1995**, *14*, 1221. (d) Chen, S.; Noll, B. C.; Peslherbe, L.; DuBois, M. R. *Organometallics* **1997**, *16*, 1089.

time scale. Each signal shows coupling with several other nuclei, suggesting additional intramolecular C−H···F "through-space" coupling.[25] Indeed, upon cooling to 258 K the indolyl signals in the ^{1}H NMR spectrum of **4c** shifted to higher field and the signal shape indicated coupling with fluorine (Figure 3).

Strong interaction with the counterion often results in a decreased catalytical activity and reduced molar mass of the polymer.[20,25,26] These findings are in agreement with the observed inactivity of mixtures composed of [**L$_2$**]Ln(CH_2SiMe_3)$_2$ and *N*-[tris(pentafluorophenyl)borane]-3*H*-indole (**C**). Strong coordination of the anion competes with the coordination of ethylene at the active site and deactivates the "catalyst".

All of the active catalyst mixtures produced linear polyethylene with molecular weights (M_w) ranging from 3.3×10^5 to 8.2×10^5. Significantly higher molecular weights were obtained for the Sc-based catalysts (Table 1, runs 1 and 3), while lower polydispersities ($M_w/M_n = 1.97-2.04$) could be achieved with the less active lutetium catalysts (Table 1, runs 2 and 4). Monomodal molecular weight distributions indicate the presence of a single active species.

In contrast to the bis(alkyl) imino-amido-pyridine precursors [**L$_2$**]Ln(CH_2SiMe_3)$_2$ (**3**), complexes [**L$_1$**]Ln(CH_2SiMe_3)(THF)$_x$ (**2**) were inactive in the polymerization of ethylene. The dianionic nature of the diamido pyridine ancillary ligand (**L$_1$**) allows for only one further alkyl ligand being removed when adding the alkyl-abstracting borate/borane compounds. Most likely, the lack of an initiating alkyl group combined with high instability of the produced species (NMR experiments showed immediate decomposition) prevents the initiation of polymerization.

Polymerization Studies with Styrene and Methyl Methacrylate. Catalyst mixtures **3**/[Ph_3C][$B(C_6F_5)_4$] were further investigated in the homopolymerization of styrene as well as copolymerization of ethylene and styrene. Attempted homopolymerization of styrene was carried out at 25 °C in 12 mL of toluene (21 μmol cat./21 μmol cocat./10.5 mmol styrene). No polymeric material could be obtained after 1.5 h. The copolymerization experiments were carried out in a 300 mL stainless steel reactor with a styrene solution in toluene at 25 °C. None of the cationic lanthanide complexes under investigation initiated the copolymerization of ethylene and styrene. Moreover, no homopolymerization of ethylene was observed even though these catalyst mixtures had shown catalytic activity in the absence of styrene. Monitoring the reaction of *in situ* formed cationic species **4a** with 1 equiv of styrene by ^{1}H and ^{13}C NMR spectroscopy showed no evidence for an interaction between the cationic rare-earth-metal center and the olefinic bond. Due to extensive overlap of the aromatic signals, π-coordination of styrene to the electron-deficient lanthanide cation cannot be precluded and might inhibit further monomer coordination and catalytic activity. (See Supporting Information Figure S4.)

Motivated by the promising catalytic behavior of [**L$_1$**]Sc(CH_2SiMe_3)(THF) (**2a**) in the polymerization of methyl methacrylate (MMA)[10] the initiating performance of corresponding neutral complexes [**L$_2$**]Ln(CH_2SiMe_3)$_2$ (**3**) as well as binary catalyst mixtures **3**/**A** and **3**/**B** has been investigated. However, under the same polymerization conditions only traces of polymeric product (PMMA) could be isolated from the reaction mixtures. Once again, these findings underline the pronounced sensitivity of closely related compounds **2** and **3** to steric and electronic modifications.

Conclusions

A series of structurally related mono(alkyl) diamido-pyridine and bis(alkyl) imino-amido-pyridine lanthanide complexes have been synthesized, and their initiating performance in the polymerization of ethylene has been studied. While neutral alkyl complexes were inactive, cationic compounds bearing the imino-amido-pyridine ligand polymerized ethylene with moderate activities. The initiating performance is governed by the lanthanide metal size (Sc > Lu) and the nature of the cocatalyst. Routinely used borate cocatalysts [Ph_3C][$B(C_6F_5)_4$] and [$PhNMe_2H$][$B(C_6F_5)_4$] yielded polyethylene, while cationization with *N*-[tris(pentafluorophenyl)borane]-3*H*-indole gave inactive species, most likely due to π-coordination of the [B(indolyl)-$(C_6F_5)_3$] anion to the cationic lanthanide metal center. Generally, the activity/inactivity of the investigated catalysts in ethylene polymerization is sensitively influenced by the presence of species strongly coordinating to the electron-deficient cationic lanthanide metal center. The availability of an initiating alkyl group is essential to provide catalytic performance, as supported by the complete inactivity of cationic species derived from the dianionic diamido-pyridine ligand. In contrast, the homopolymerization of MMA is only initiated by the neutral mono(alkyl) diamido-pyridine complexes. Neither the neutral bis(alkyl) imino-amido-pyridine complexes nor their cationic variants gave positive polymerization protocols.

Experimental Section

General Considerations. All operations were performed with rigorous exclusion of air and water, using standard Schlenk, high-vacuum, and glovebox techniques (MBraun MBLab; <1 ppm O_2, <1 ppm H_2O). Hexane and toluene were purified by using Grubbs columns (MBraun SPS, solvent purification system) and stored in a glovebox. CD_2Cl_2 was obtained from Aldrich, vacuum transferred from calcium hydride, and degassed. [$PhNMe_2H$][$B(C_6F_5)_4$] and [Ph_3C][$B(C_6F_5)_4$] were purchased from Boulder Scientific Company and used without further purification. $LnCl_3(THF)_x$,[27] $LiCH_2SiMe_3$,[28] $Ln(CH_2SiMe_3)_3(THF)_2$,[29] 2-{(2,6-*i*$Pr_2C_6H_3$)N=CMe}−6-{(2,6-*i*$Pr_2C_6H_3$)NHCMe$_2$}C_5H_3N] (H**L$_2$**),[30] [**L$_1$**]Ln(CH_2SiMe_3)-(THF)$_x$ (**2**),[10] [2-{2,6-*i*$Pr_2C_6H_3$)N=CMe}-6-{(2,6-*i*$Pr_2C_6H_3$)NC-Me$_2$}C_5H_3N]Lu(CH_2SiMe_3)$_2$ (**3b**),[13] and *N*-[tris(pentaflourophenyl)borane]-3*H*-indole[21] were prepared according to literature procedures. The NMR spectra of air- and moisture-sensitive compounds were recorded by using J. Young valve NMR tubes at 25 °C on a Varian UI 300 MHz, a Bruker-AVANCE-DMX400 (5 mm BB, ^{1}H: 400.13 MHz; ^{13}C: 100.62 MHz), and a Bruker-BIOSPIN-AV500 (5 mm BBO, ^{1}H: 500.13 MHz; ^{13}C: 125.77 MHz). ^{1}H and ^{13}C shifts are referenced to internal solvent resonances and reported in parts per million relative to TMS. ^{11}B NMR (161 MHz) spectra were referenced to an external standard of boron trifluoride diethyl etherate (0.0 ppm, C_6D_6). ^{19}F NMR spectra (471 MHz) are referenced to external $CFCl_3$. IR spectra were recorded on a Nicolet Impact 410 FTIR spectrometer as Nujol mulls sandwiched between CsI plates. Elemental analyses were performed on an Elementar Vario EL III.

(25) Focante, F.; Camurati, I.; Resconi, L.; Guidotti, S.; Beringhelli, T.; D'Alfonso, G.; Donghi, D.; Maggioni, D.; Mercandelli, P.; Sironi, A. *Inorg. Chem.* **2006**, *45*, 1683.

(26) Hayes, P. G.; Piers, W. E.; Parvez, M. *J. Am. Chem. Soc.* **2003**, *125*, 5622.

(27) Anwander, R. *Top. Organomet. Chem.* **1999**, *2*, 1.

(28) Hultzsch, K. C. Ph.D. Thesis, Johannes Gutenberg-Universität Mainz, 1999.

(29) Lappert, M. F.; Pearce, R. *J. Chem. Soc., Chem. Commun.* **1973**, 126.

(30) Bruce, M.; Gibson, V. C.; Redshaw, C.; Solan, G. A.; White, A. J. P.; Williams, D. J. *Chem. Commun.* **1998**, 2523.

[2-{(2,6-*i*Pr$_2$C$_6$H$_3$)N═CMe}-6-{(2,6-*i*Pr$_2$C$_6$H$_3$)NCMe$_2$}C$_5$H$_3$N]-Sc(CH$_2$SiMe$_3$)$_2$ (3a). To a stirred solution of Sc(CH$_2$SiMe$_3$)$_3$(THF)$_2$ (517 mg, 1.15 mmol) (**1a**) in 8 mL of toluene was added a solution of yellow H**L$_2$** (571 mg, 1.15 mmol) in 15 mL of toluene, affording an immediate red color change. The resulting mixture was stirred for 3 h and then concentrated to approximately 15 mL. Cooling the red solution to −30 °C overnight gave red microcrystals of **3a**, which were isolated by filtration, washed with hexane, and dried under vacuum (758 mg, 1.06 mmol, 92% isolated yield). IR (Nujol): 1582 s (C═N), 1458 vs (Nujol), 1385 vs (Nujol), 1303 s, 1251 m, 1240 w, 1204 w, 1158 m, 1137 w, 1111 w, 1090 w, 1059 w, 1013 w, 1002 w, 976 w, 940 w, 857 m, 826 w, 764 m, 733 s, 676 w, 572 w, 536 w cm^{-1}. ^{1}H NMR (500 MHz, CD$_2$Cl$_2$, −50 °C): δ 8.12 (t, ^3J = 8.0 Hz, 1 H, C$_5$H$_3$N-*p*-proton), 7.87 (d, ^3J = 7.5 Hz, 1 H, C$_5$H$_3$N-*m*-proton), 7.81 (d, ^3J = 8.4 Hz, 1 H, C$_5$H$_3$N-*m*-proton), 7.28−7.02 (m, 6 H, ar), 4.22 (m, 1 H, ar-CH), 3.12 (m, 1 H, ar-CH), 2.86 (m, 1 H, ar-CH), 2.64 (m, 1 H, ar-CH), 2.35 (s, 3 H, N═CCH$_3$), 1.64 (s, 3 H, NCCH$_3$), 1.30 (d, ^3J = 6.3 Hz, 3 H, CH$_3$), 1.21 (m, 12 H, CH$_3$), 1.10 (s, 3 H, NCCH$_3$), 1.03 (d, ^3J = 6.3 Hz, 3 H, CH$_3$), 1.01 (d, ^3J = 6.3 Hz, 3 H, CH$_3$), 0.90 (d, ^3J = 6.3 Hz, 3 H, CH$_3$), 0.04 (s, 2 H, Sc-CH$_2$), −0.51 (s, 9 H, Si-CH$_3$), −0.77 (s, 9 H, Si-CH$_3$), −1.02 (s, 2 H, Sc-CH$_2$) ppm. ^{13}C{^{1}H} NMR (125 MHz, CD$_2$Cl$_2$, 25 °C): δ 177.3, 175.3, 150.2, 148.7, 147.8, 143.0, 140.7, 139.7, 129.5, 128.7, 127.5, 126.1, 125.8, 125.2, 123.8, 123.3, 122.3, 68.7, 43.5, 29.4, 28.2, 27.6, 25.2, 24.3, 20.5, 3.4 ppm. Anal. Calcd for C$_{42}$H$_{68}$N$_3$Si$_2$Sc: C, 70.44; H, 9.57; N, 5.87. Found: C, 70.83; H, 9.28; N, 5.82.

[2-{(2,6-*i*Pr$_2$C$_6$H$_3$)N═CMe}-6-{(2,6-*i*Pr$_2$C$_6$H$_3$)NCMe$_2$}C$_5$H$_3$N]-Y(CH$_2$SiMe$_3$)$_2$ (3c). To a stirred solution of Y(CH$_2$SiMe$_3$)$_3$(THF)$_2$ (287 mg, 0.58 mmol) (**1c**) in 5 mL of toluene was added a solution of yellow H**L$_2$** (289 mg, 0.58 mmol) in 5 mL of toluene, affording an immediate red color change. The resulting mixture was stirred for 4 h and then concentrated to approximately 5 mL. Cooling the red solution to −30 °C overnight gave red microcrystals of **3c**, which were isolated by filtration, washed with hexanes, and dried under vacuum (140 mg, 0.18 mmol, 32% isolated yield). IR (Nujol): 1582 s (C═N), 1468 vs (Nujol), 1375 vs (Nujol), 1308 s, 1282 m, 1251 m, 1235 w, 1204 w, 1095 w, 1049 w, 1013 w, 982 w, 935 w, 857 s, 821 w, 795 m, 769 m, 728 s, 671 w, 567 w, 531 w cm^{-1}. ^{1}H NMR (400 MHz, CD$_2$Cl$_2$, −50 °C): δ 8.12 (t, ^3J = 7.6 Hz, 1 H, C$_5$H$_3$N-*p*-proton), 7.89 (d, ^3J = 7.6 Hz, 1 H, C$_5$H$_3$N-*m*-proton), 7.81 (d, ^3J = 7.6 Hz, 1 H, C$_5$H$_3$N-*m*-proton), 7.31−7.03 (m, 6 H, ar), 4.27 (m, 1 H, ar-CH), 3.00 (m, 1 H, ar-CH), 2.88 (m, 1 H, ar-CH), 2.58 (m, 1 H, ar-CH), 2.36 (s, 3 H, N═CCH$_3$), 1.71 (s, 3 H, NCCH$_3$), 1.33 (s, 3 H, NCCH$_3$), 1.23 (s br, 6 H, CH$_3$), 1.18 (s br, 6 H, CH$_3$), 1.11 (s br, 3 H, CH$_3$), 1.02 (s br, 3 H, CH$_3$), 0.93 (s br, 6 H, CH$_3$), −0.40 (s, 9 H, Si-CH$_3$), −0.58 (d, ^2J = 9.2 Hz, 1 H, Y-CH$_2$), −0.71 (s, 9 H, Si-CH$_3$), −0.99 (d, ^2J = 11.2 Hz, 1 H, Y-CH$_2$), −1.47 (d, ^2J = 11.2 Hz, 1 H, Y-CH$_2$), −1.68 (d, ^2J = 9.2 Hz, 1 H, Y-CH$_2$) ppm. ^{13}C{^{1}H} NMR (101 MHz, CD$_2$Cl$_2$, 25 °C): δ 178.8, 177.0, 150.5, 149.2, 146.8, 140.8, 139.5, 129.5, 128.7, 127.9, 125.7, 125.2, 123.6, 123.4, 122.9, 70.9, 67.8, 36.2, 29.4, 28.8, 28.3, 27.4, 25.2, 24.3, 20.5, 3.8, 1.4, 0.2 ppm. Anal. Calcd for C$_{42}$H$_{68}$N$_3$Si$_2$Y: C, 66.37; H, 9.02; N, 5.53. Found: C, 66.04; H, 9.12, N, 5.09.

Synthesis of {[L$_2$]Lu(CH$_2$SiMe$_3$)}$^+${B(C$_6$F$_5$)$_4$}$^-$ (4a) from [L$_2$]Lu(CH$_2$SiMe$_3$)$_2$ (3b) and [Ph$_3$C][B(C$_6$F$_5$)$_4$] (A). In a glovebox, **3b** (11 mg, 0.01 mmol) and **A** (11 mg, 0.01 mmol) were placed in a J. Young valve NMR tube, and 0.5 mL of C$_6$D$_5$Cl or CD$_2$Cl$_2$, respectively, was added. ^{1}H NMR (500 MHz, C$_6$D$_5$Cl, 25 °C): δ 7.83 (t, ^3J = 6.0 Hz, 1 H, C$_5$H$_3$N-*p*-proton), 7.63 (d, ^3J = 6.0 Hz, 1 H, C$_5$H$_3$N-*m*-proton), 7.40 (d, ^3J = 6.0 Hz, 1 H, C$_5$H$_3$N-*m*-proton), 7.33−6.97 (m, 21 H, ar, Ph), 5.56 (s, Ph$_3$C*H*), 3.60 (m, 2 H, ar-CH), 2.63 (m, 2 H, ar-CH), 2.20 (s, 3 H, N═CCH$_3$), 2.19 (s, Si−C*H*$_2$), 2.10 (s, Si−C*H*$_2$), 1.49 (s, 6 H, NCCH$_3$), 1.30 (d, ^3J = 5.2 Hz, 6 H, CH$_3$), 1.23 (d, ^3J = 5.2 Hz, 6 H, CH$_3$), 1.10 (d, ^3J = 5.2 Hz, 6 H, CH$_3$), 1.03 (d, ^3J = 5.2 Hz, 6 H, CH$_3$), 0.01 (Si-C*H*$_3$), −0.15 (s, 9 H, Si-C*H*$_3$), −0.30 (Si−C*H*$_3$), −0.44 (s br, 2 H, Lu-C*H*$_2$) ppm. ^{1}H NMR (500 MHz, CD$_2$Cl$_2$, 25 °C): δ 8.21 (t, ^3J = 8.0 Hz, 1 H, C$_5$H$_3$N-*p*-proton), 7.96 (d, ^3J = 8.0 Hz, 1 H, C$_5$H$_3$N-*m*-proton), 7.89 (d, ^3J = 8.0 Hz, 1 H, C$_5$H$_3$N-*m*-proton), 7.33−7.08 (m, 6 H, ar), 3.63 (m, 2 H, ar-CH), 2.85 (m, 2 H, ar-CH), 2.41 (s, 3 H, N═CCH$_3$), 1.47 (s, 6 H, NCCH$_3$), 1.27 (d, ^3J = 6.5 Hz, 6 H, CH$_3$), 1.20 (d, ^3J = 6.5 Hz, 6 H, CH$_3$), 1.17 (d, ^3J = 6.5 Hz, 6 H, CH$_3$), 1.11 (d, ^3J = 6.5 Hz, 6 H, CH$_3$), −0.02 (s, 9 H, Si−C*H*$_3$), −0.32 (s br, 2 H, Lu-C*H*$_2$) ppm. ^{13}C{^{1}H} NMR (126 MHz, C$_6$D$_6$, 25 °C): δ 179.0, 149.5, 141.7, 141.4, 140.0, 129.9, 129.6, 129.5, 128.9, 128.7, 128.2, 126.5, 125.8, 125.0, 124.6, 123.9, 123.6, 68.9, 54.5, 31.0, 29.6, 28.5, 27.4, 24.9, 23.9, 19.6, 3.5, 0.2, −2.0 ppm. ^{11}B{^{1}H} NMR (161 MHz, C$_6$D$_5$Cl, 25 °C): δ −16.2 (s) ppm. ^{19}F NMR (471 MHz, C$_6$D$_5$Cl, 25 °C): δ −131.6 (d, *o*-F), −162.4 (t, *p*-F), −166.4 (t, *m*-F) ppm.

Reaction of LiCH$_2$SiMe$_3$ and Ph$_3$CCl. In a glovebox, LiCH$_2$SiMe$_3$ (3 mg, 0.03 mmol) and Ph$_3$CCl (8 mg, 0.03 mmol) were placed in a J. Young valve NMR tube, and 0.5 mL of C$_6$D$_5$Cl was added. ^{1}H NMR (400 MHz, C$_6$D$_5$Cl, 25 °C): δ 7.44−7.09 (overlapping m, Ph), 5.56 (s, Ph$_3$C*H*), 2.19 (s, Si-C*H*$_2$), 2.10 (s, Si-C*H*$_2$), 0.01 (Si-C*H*$_3$), −0.30 (Si-C*H*$_3$) ppm.

Synthesis of {[L$_2$]Lu(CH$_2$SiMe$_3$)}$^+${B(C$_6$F$_5$)$_4$}$^-$ (4b) from [L$_2$]Lu(CH$_2$SiMe$_3$)$_2$ (3b) and [PhNMe$_2$H][B(C$_6$F$_5$)$_4$] (B). In a glovebox, **3b** (15 mg, 0.02 mmol) and **B** (13 mg, 0.02 mmol) were placed in a J. Young valve NMR tube, and 0.5 mL of C$_6$D$_5$Cl was added. ^{1}H NMR (400 MHz, C$_6$D$_5$Cl, 25 °C): δ 7.83 (t, ^3J = 7.5 Hz, 1 H, C$_5$H$_3$N-*p*-proton), 7.66 (d, ^3J = 7.5 Hz, 1 H, C$_5$H$_3$N-*m*-proton), 7.41 (d, ^3J = 7.5 Hz, 1 H, C$_5$H$_3$N-*m*-proton), 7.36−7.12 (m, 11 H, ar, Ph), 2.70 (s br, 6 H, N(CH$_3$)$_2$, 2.66 (m, 4 H, ar-CH), 2.24 (s, 3 H, N═CCH$_3$), 1.46 (s, 6 H, NCCH$_3$), 1.41 (d, ^3J = 6.5 Hz, 6 H, CH$_3$), 1.29 (d, ^3J = 6.5 Hz, 6 H, CH$_3$), 1.23 (d, ^3J = 6.5 Hz, 6 H, CH$_3$), 1.10 (d, ^3J = 6.5 Hz, 6 H, CH$_3$), 0.00 (s, Si(C*H*$_3$)$_4$), −0.08 (s, 9 H, Si-C*H*$_3$), −0.47 (s br, 2 H, Lu-C*H*$_2$) ppm. ^{13}C{^{1}H} NMR (126 MHz, C$_6$D$_5$Cl, 25 °C): δ 180.0, 150.0, 148.1, 142.1, 139.8, 138.0, 136.0, 129.9, 125.3, 117.1, 112.7, 72.5, 40.4, 32.1, 30.4, 28.5, 27.5, 24.7, 24.4, 23.2, 19.7, 3.6, 0.2, −1.4, ppm. ^{11}B{^{1}H} NMR (161 MHz, C$_6$D$_5$Cl, 25 °C): δ −16.3 (s) ppm. ^{19}F NMR (471 MHz, C$_6$D$_5$Cl, 25 °C): δ −131.4 (d, *o*-F), −162.4 (t, *p*-F), −166.2 (t, *m*-F) ppm.

Synthesis of {[L$_2$]Lu(CH$_2$SiMe$_3$)}$^+${B(indolyl)(C$_6$F$_5$)$_3$}$^-$ (4c) from [L$_2$]Lu(CH$_2$SiMe$_3$)$_2$ (3b) and *N*-[tris(pentafluorophenyl)borane]-3*H*-indole (C). In a glovebox, **3b** (13 mg, 0.01 mmol) and **C** (9 mg, 0.01 mmol) were placed in a J. Young valve NMR tube, and 0.5 mL of C$_6$D$_5$Cl was added. ^{1}H NMR (400 MHz, C$_6$D$_5$Cl, 25 °C): δ 7.80 (d, ^3J = 7.6 Hz, 1 H, C$_5$H$_3$N-*m*-proton), 7.71 (s br, 1 H, H2), 7.38−6.97 (m, 9 H, ar, C$_5$H$_3$N-*p*-proton, C$_5$H$_3$N-*m*-proton, H7), 6.50 (s br, 1 H, H4), 6.35 (s br, 1 H, H6), 6.06 (s br, 1 H, H5), 5.73 (s br, 1 H, H3), 3.76 (m, 1 H, ar-CH), 3.07 (m, 1 H, ar-CH), 2.65 (m, 1 H, ar-CH), 2.43 (m, 1 H, ar-CH), 1.61 (s, 3 H, N═CCH$_3$), 1.59 (s, 6 H, NCCH$_3$), 1.26 (m, 6 H, CH$_3$), 1.09 (d, ^3J = 5.4 Hz, 3 H, CH$_3$), 0.99 (m, 12 H, CH$_3$), 0.69 (d, ^3J = 4.7 Hz, 3 H, CH$_3$), 0.01 (s, Si(C*H*$_3$)$_4$), −0.04 (s br, 2 H, Lu-C*H*$_2$), −0.28 (s, 9 H, Si-C*H*$_3$) ppm. ^{13}C{^{1}H} NMR (126 MHz, C$_6$D$_5$Cl, 25 °C): δ 181.1, 178.2, 149.7, 148.8, 139.9, 139.2, 137.9, 135.9, 127.0, 125.7, 125.0, 123.9, 122.1, 119.3, 72.4, 69.6, 69.2, 68.2, 32.1, 30.4, 28.5, 27.4, 25.1, 24.8, 23.2, 19.8, 3.6, 3.3, 0.2 ppm. ^{11}B{^{1}H} NMR (161 MHz, C$_6$D$_5$Cl, 25 °C): δ −8.4 (s br) ppm. ^{19}F NMR (471 MHz, C$_6$D$_5$Cl, 25 °C): δ −126.4 (m, *o*-F), −129.4 (m, *o*-F), −131.6 (m, *o*-F), −134.4 (m, *o*-F),−159.1 (m, *p*-F), −160.3 (m, *p*-F), −163.7 (m, *m*-F), −164.2 (m, *m*-F), −164.9 (m, *m*-F), −166.0 (m, *m*-F) ppm.

Ethylene Polymerization. The Parr reactor was flushed 3−4 times with ethylene. In a nitrogen-filled glovebox an injector was charged with a solution of the borate activator (0.01 mmol) in 30 mL of toluene. This was injected into the reactor under ethylene pressure. The solution was heated to 25 °C and overpressurized with ethylene to a total pressure of 150 psi. The solution was

equilibrated at 25 °C under constant ethylene pressure for at least 20 min. The catalyst (0.01 mmol) was dissolved in 20 mL of toluene, added into an injector, and injected into the reactor under ethylene pressure. Immediately prior to catalyst injection the ethylene line was disconnected and the pressure in the reactor was reduced by 60 psi to provide the pressure differential and allow the catalyst solution to flow into the reactor. The ethylene hose was reconnected immediately after catalyst injection. The reaction was run for 1 h at constant pressure and temperature; it was then quenched by injection of methanol (10 mL), and the reactor was slowly vented and opened. The polymer was precipitated in 400 mL of acidified methanol (5% HCl), filtered, washed with methanol, and dried under vacuum at 40 °C to a constant weight. Polymer molecular weights and molecular weight distributions were determined by the high-temperature gel permeation chromatography using polyethylene for GPC calibration. A Varian UI 300 spectrometer was used to perform ^{13}C NMR measurements. The polymer samples were prepared by dissolving 100−200 mg of polymer in 3 mL of *o*-dichlorobenzene/10 vol % benzene-d_6 in a 10 mm NMR tube. The spectra were measured at 100 °C using acquisition times = 1 s, additional delays = 5 s, and gated proton decoupling.

Acknowledgment. Financial support from the Bayerische Forschungsstiftung, the Norwegian Research Council, the Deutsche Forschungsgemeinschaft (SPP 1166), and the NSF (CHE-0611563) is gratefully acknowledged. We thank Lutz H. Gade and Rich Jordan for stimulating discussions.

Supporting Information Available: ^1H NMR spectra of the soluble decomposition products of **3a**, **3b**/$[Ph_3C][B(C_6F_5)_4]$ in CD_2Cl_2, **3b**/$[PhNMe_2H][B(C_6F_5)_4]$ in chlorobenzene-d_5, and **3b**/$[Ph_3C][B(C_6F_5)_4]$ with 1 equiv of styrene, and a CIF file giving full crystallographic data for **3a**. This material is available free of charge via the Internet at http://pubs.acs.org.

OM701195X